

Radioactive Decay Lines from Asymmetric Supernova Explosions

A. Hungerford^{a,b}

^a*Los Alamos National Laboratory*

^b*Steward Observatory - University of Arizona*

Abstract

High energy emission from supernovae provide a direct window into the quantity and distribution of radioactive elements produced in these explosions. Combining supernova explosion calculations with 3D Monte Carlo γ -ray transport, I have studied the effect mixing and asymmetries have on the hard X-ray and γ -ray spectra. With sufficient spectral resolution, the emission line profiles from Nickel decay have enough information to distinguish between spherical and mildly asymmetric supernova explosions.

Key words: Gamma-rays, Supernovae, Asymmetries

PACS: 95.85.Pw, 97.60.Bw

1 Introduction

The past decade has brought great strides in observational and theoretical studies of core-collapse supernovae, with interest stimulated by the wealth of data (and surprises) obtained from SN 1987A. For theoretical work in particular, the early emergence of hard X- and γ -ray emission from SN 1987A (X-rays: e.g. Dotani et al. 1987; γ -rays: e.g. Cook et al. 1988; Mahoney et al. 1988; Matz et al. 1988) signaled a departure from the spherically symmetric geometry that had been assumed in models of core-collapse explosions to that point. The appearance of this high energy emission, nearly 6 months earlier than theorists had predicted, was most readily explained by the outward mixing of the Nickel synthesized in the inner layers of the explosion (e.g. Pinto & Woosley 1988b, Arnett et al. 1989 and references therein). In addition, line profiles from Iron (the daughter product of Nickel decay) were broadened to roughly 3500 km/s (Spyromilio, Meikle & Allen 1990), further evidence that Nickel had been mixed to large radii in the homologous supernova ejecta. This

qualitative explanation for the observations motivated several groups to investigate, at a detailed level, the multidimensional instabilities which give rise to such mixing within the context of massive star explosions (Arnett, Fryxell, & Müller 1989; Hachisu et al. 1990; Herant & Benz 1992; Kifonidis et al. 2000). The hydrodynamical simulations carried out by these groups resulted in extended spatial distributions of the Nickel, but not sufficiently extended to match the line profiles of the iron emission from SN 1987A.

A variety of ways to enhance the mixing in theoretical calculations, thus bringing them into agreement with observations, were proposed by Herant & Benz (1992): (1) the decay of ^{56}Ni could inject enough energy to force additional mixing, (2) convection in the pre-collapse core could seed more vigorous mixing and (3) global asymmetries in the explosion mechanism itself could enhance mixing along a particular direction in the explosion. This third possibility has been invoked to explain several other observational puzzles regarding core-collapse events. Nagataki et al. (1998) found that not only could slight asymmetries in the supernova explosion produce the required mixing to explain 1987A, but they could also explain anomalies in the nucleosynthetic yields produced by several supernovae. Furthermore, the most straightforward explanation of the large polarization seen in core-collapse supernovae (see Leonard & Filippenko 2001 and references therein) is that the explosion driving these supernovae is inherently asymmetric (Höflich 1991). In addition, the high observed velocities of pulsars and the formation scenarios of neutron star binaries both suggest that neutron stars are given strong kicks at birth. These kicks are most easily explained by some asymmetry in the supernova explosion where the neutron star is born (see Fryer, Burrows, & Benz 1996 for a review).

In this proceeding, we present theoretical γ -ray spectra calculated using asymmetric supernova models as input to a Monte Carlo γ -ray transport code. The asymmetry of the input model is motivated by the strong asymmetries that stellar rotation has been shown to produce in the supernova explosion (Mönchmeyer & Müller 1989; Janka & Mönchmeyer 1989; Fryer & Heger 2000, Khokhlov et al. 1999). The nature of these asymmetries depends upon the angular momentum profile of the collapsing star and, although most calculations predict jet-like explosions along the rotation axis, some calculations imply that an equatorial explosion could occur (Mönchmeyer & Müller 1989). Our spectral calculations were carried out for both a jet-like explosion with axis ratio of 2:1 (motivated by Fryer & Heger 2000; we refer to this explosion model as Jet2) and a symmetric explosion model (Symmetric). Our analysis of these model spectra concentrates on the differences in total luminosity and line profile shape with the introduction of realistic explosion asymmetries. Since the progenitor star used as input to our simulations was a $15 M_{\odot}$ red supergiant, we are unable to directly compare our calculated spectra with the observed high energy spectra of SN 1987A. However, we discuss how our models compare to various spectral trends observed from SN 1987A.

2 γ -ray Line Profiles

The high energy spectra were calculated using a Monte Carlo technique, similar to that described in Ambwani & Sutherland 1988, for modelling γ -ray transport in 3-dimensions. Input models of the supernova ejecta (element abundances, density and velocities) were taken from 3-dimensional SPH explosion simulations (Hungerford, Fryer & Warren 2003; models Jet2 and Symmetric) and mapped onto a $140 \times 140 \times 140$ cartesian grid. Escaping photons were tallied into 250 coarse energy bins, with finer binning at the decay line energies to provide line profile information. The emergent photons were also tallied into 11 angular bins ($\Delta\theta = 10^\circ$) along the polar axis (the models investigated in this work are essentially axisymmetric, alleviating the need to tally in azimuthal angle as well.)

A detailed look at the γ -ray line profile shapes and strengths, for the 1.238 and 0.847 MeV ^{56}Co lines, reveals clear trends with viewing angle. Figure 1 shows line profiles of the 0.847 MeV ^{56}Co line for both the Symmetric and Jet2 explosion models. We have placed this object at the distance of the Large Magellanic Cloud (60 kpc) for easy comparison with flux data from SN 1987A observations. The broadening of the line is caused by Doppler velocity shifts resulting from the spatial distribution of radioactive nickel in the homologously expanding ejecta. The 4 panels shown are for days 200, 250, 300, and 365 after explosion. The three lines in the Jet2 spectra represent different viewing angles through the ejecta (along the pole, the equator and an intermediate angle $\sim 45^\circ$.) For the Symmetric spectra, we have plotted these same viewing angles.

As we can see from the above figure, both explosion scenarios (Symmetric and Jet2) show blue-shifted line profiles, though to varying degree. These differences can be best understood by examining the physical effects which dictate the formation of the line profile edges. The blue edge to the lines is set by the maximum observed line of sight velocity of the ^{56}Co in the ejecta. Since the expansion is basically homologous after 100 days, the line of sight velocity of a fluid element in the ejecta is proportional to its distance above the mid-plane of the explosion. Each spectral energy bin in the line profile can be mapped to a unique line of sight velocity in the ejecta, which can in turn be mapped to a specific height above the mid-plane. For example, defining the line of sight to be along the z-axis, the line profile shape should be proportional to the total mass of Cobalt summed in x and y as a function of z height in the ejecta. Therefore, the bluest edge of the line will arise from material that was mixed furthest out along the line of sight direction.

Figure 2 shows a contour plot of density (outer contour) and ^{56}Co number density (inner contour) for the Jet2 and Symmetric models at $t = 150$ days.

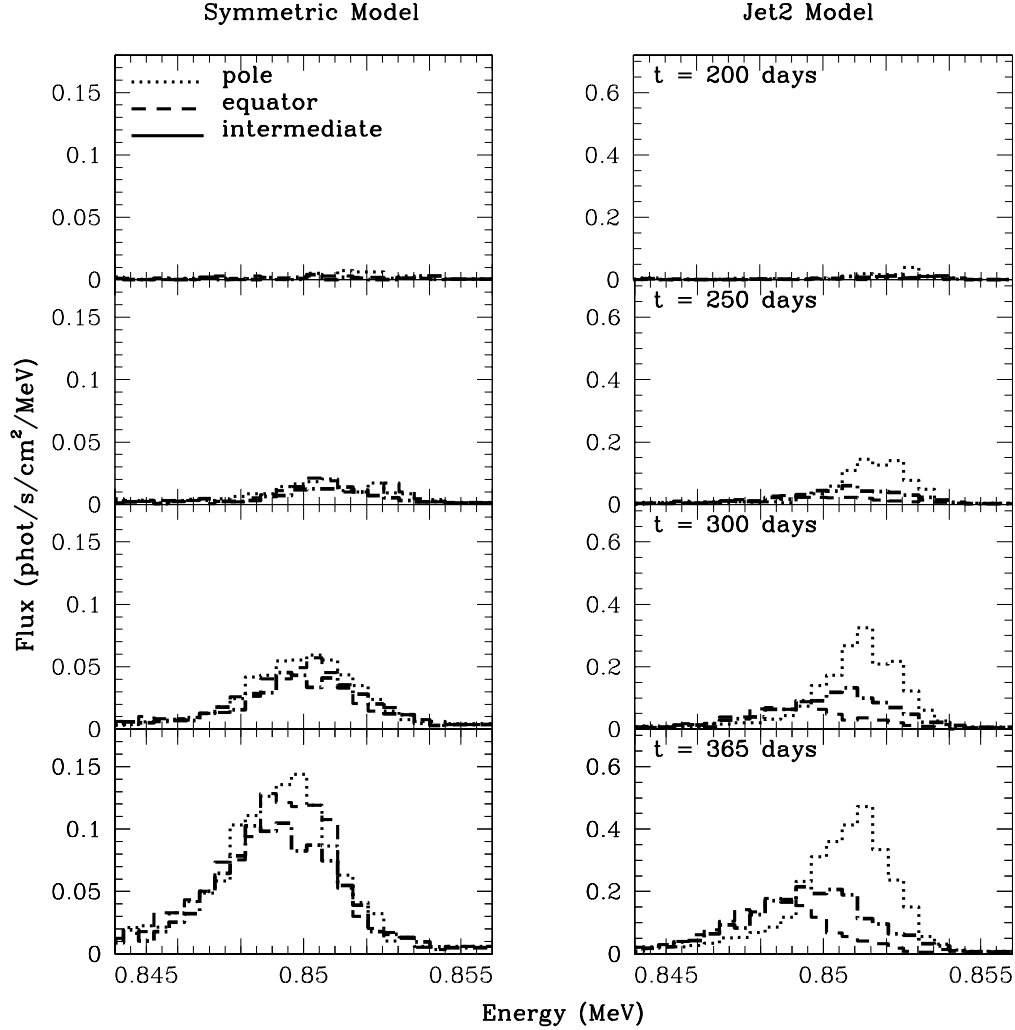


Fig. 1. Line profiles of the ^{56}Co 0.847 MeV line for both the Symmetric (left panel) and Jet2 (right panel) models at 4 different times during the explosion (200, 250, 300, 365 days). 3 different viewing angles are shown: polar view (dotted lines), equatorial view (dashed lines) and an intermediate view angle of $\sim 45^\circ$ (dash-dot lines). The flux axis for the Jet2 explosion is scaled by a factor of 4 over the Symmetric model.

Decay of ^{56}Co is the major source of γ -ray photons, so the inner contour essentially traces the surface of the emission region. The horizontal and vertical lines in Figure 2 represent lines of sight from the ejecta surface to the emission source and are labeled with the optical depth along that line of sight. The dominant opacity for the hard X- and γ -rays is Compton scattering off electrons and, since the density contours remain roughly spherical in both models, the optical depth from a given point to the ejecta surface is roughly constant.

It is clear from Figure 2 that the nickel was mixed further out in the polar direction (z -axis of Figure 2) of the asymmetric explosion. Following the arguments above, it is not surprising that the γ -ray line profiles viewed along the polar direction are much more blueshifted for the Jet2 model than the

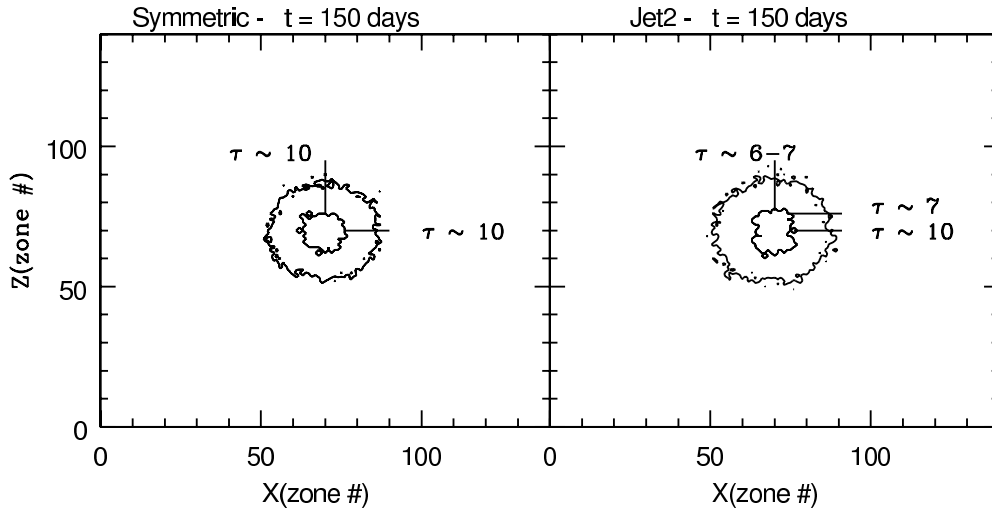


Fig. 2. Contour plots in the xz -plane of the Symmetric and Jet2 explosion models at $t = 150$ days. Inner contour is for ^{56}Co number density which traces the surface of the γ -ray emitting region. Outer contour is for the mass density which follows electron density and thus traces the dominant opacity source (Compton scattering). The lines represent lines-of-sight through the ejecta for which the optical depth from emission region to ejecta surface has been calculated. Regardless of viewing angle, the optical depth of the ^{56}Co ejected along the poles in the Jet2 explosion remains quite low. Hence, it is this material that dominates the observed emission for all viewing angles in the aspherical explosion.

Symmetric model. Figure 2 does not show a very large difference in the extent of mixing along the equatorial direction between the two models. Correspondingly, the blue edge of the Symmetric lines and the equator view of the Jet2 lines are comparable.

The red edge of the lines is determined by the escaping emission from ^{56}Co with the smallest line of sight velocity in the ejecta. In a Symmetric model, this should be an indication of how deep into the ejecta we can see along a given viewing angle. However, there is a more pronounced effect at play in the asymmetric explosion models. Much of the γ -ray emission for the equatorial view arises from the “tips” of the elongated ^{56}Co distribution. This material has a very low line of sight velocity for an equatorial observer, since it is being ejected predominantly in the polar direction. This allows for a significantly lower velocity red edge of the equator view lines, even though the optical depth profiles do not vary much between polar and equator viewing angles.

It is interesting to note that the γ -ray line profiles from SN 1987A were in fact redshifted, a trend that is not obtained with these simulations. Although the γ -ray data uncertainties were quite high, this redshift was also observed in the far infrared forbidden lines of FeII, providing verification for the γ -ray line centroid measurements. As was discussed above, the spectral line shape is directly correlated with the total Cobalt mass at a given z -coordinate along the

line of sight. With this in mind, the observed red-shifted line profiles towards SN 1987A imply, not only a break in spherical symmetry, but also a break in axisymmetry of the ejecta. Namely, there should be more Nickel/Cobalt mass on the far side of SN 1987A’s ejecta as seen from our viewing angle. Pulsar velocity distributions also support the need for some non-axisymmetry in core-collapse supernova explosions. An interesting study, which will be addressed in a future paper, is to link the magnitude of velocity kick imparted to a neutron star with the compositional asymmetry implied by the redshifted line profiles of SN 1987A.

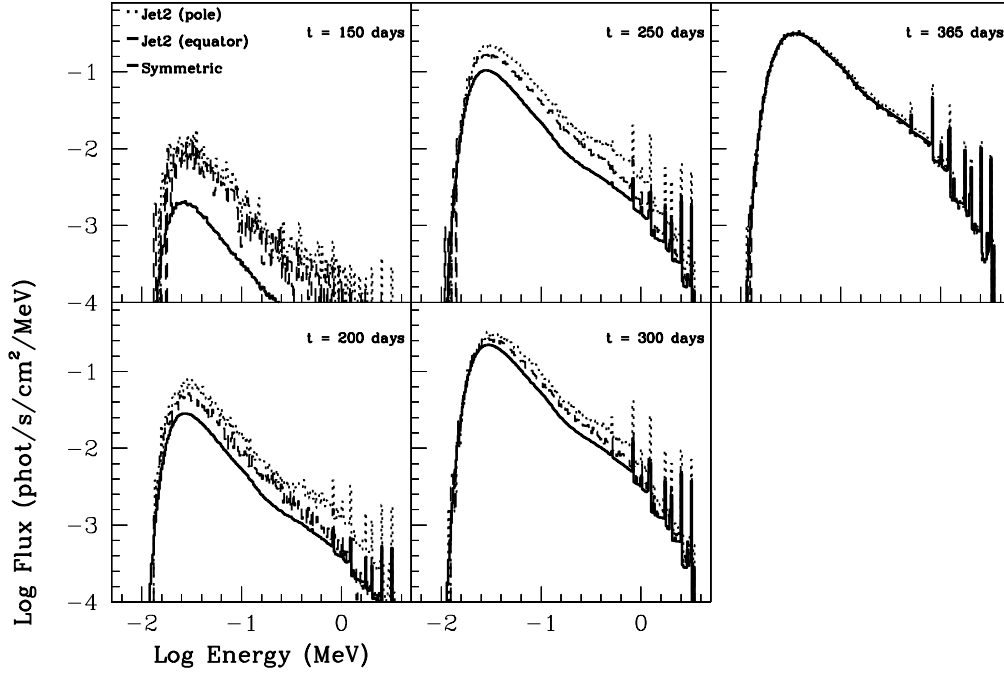


Fig. 3. Total hard X- and γ -ray spectrum at 5 different times during the explosion (150,200,250,300,365 days) for symmetric (solid lines) and aspherical (Jet2) explosions (dotted and dashed lines). The flux is determined by assuming the object is 60 kpc from the observer. The dotted lines refer to an aspherical explosion where the jet is directed along the line of sight of the observer. The dashed lines refer to an explosion where the observer line of sight is directed 90° off of the jet axis, in the equatorial direction. Regardless of observer viewing angle at early times, the aspherical explosion is measurably brighter than the symmetric explosion.

3 Hard X-ray and γ -ray Spectrum

Figure 3 is a logarithmic plot of the calculated photon flux (γ /s/MeV/cm²) across the entire energy range investigated with these simulations (0.3 keV - 4 MeV). The 5 panels are spectra from the different time slices; in each panel, we plot the spectrum for the Symmetric model, along with polar and equatorial views of the Jet2 model. The effects of mixing are present in both

these simulations, though at differing levels due to the differences in explosion asymmetry. It can be seen immediately that the hard X-rays emerge earlier from the ejecta with a global explosion asymmetry (Jet2 model). This holds regardless of viewing angle (pole versus equator) towards the explosion.

As discussed in the introduction, the observed high energy spectrum of SN 1987A differed from the predictions of theoretical onion-skin models in two fundamental ways. Both the broad lines of Nickel and the early emergence of the hard X-rays could be explained qualitatively by invoking a mixing argument. From a theoretical standpoint, including a 1D prescription for that mixing makes the assumption that both data points can be fit with one free parameter. However, the simulations in this work suggest that the addition of a global asymmetry will change the direct correlation between the emergence time and the degree of line broadening. That is to say, for a given hard X-ray flux, the Symmetric model will correspond to a single line profile, regardless of viewing angle. The Jet2 model, however, produces similar hard X-ray continua for different viewing angles, but the line profile varies significantly with viewing angle. In fact, the data for SN 1987A (the γ -line profiles and hard X-ray continuum) were not fit well by 1D models. In particular, the model 10HMM (Pinto & Woosley 1988), which was mixed sufficiently to account for the flux in the hard X-ray continuum observations, resulted in γ -line centroids that were shifted too far to the blue (Tueller et al. 1990). Although the uncertainties in this data were relatively large, this trend may be in the right direction to suggest a global asymmetry (i.e. an asymmetric explosion scenario for SN 1987A could produce the same hard X-ray flux level, but with a redder line profile than the symmetric explosion scenario).

References

- [Ambwani & Sutherland 1988] Ambwani, K. & Sutherland, P. 1988, *ApJ*, **325**, 820
- [1] Arnett, D., Fryxell, B., & Müller, E. 1989, *ApJ*, **341**, L63
- [Arnett et al. 1989] Arnett, W. D., Bahcall, J. N., Kirshner, R. P., & Woosley, S. E. 1989, *ARA&A*, **27**, 629
- [Cook et al. 1988] Cook, W. R., Palmer, D. M., Prince, T. A., Schindler, S. M., Starr, C. H., & Stone, E. C. 1988, *ApJ*, **334**, L87
- [Dotani et al. 1987] Dotani, T., Hayashida, K., Inoue, H., Itoh, M., & Koyama, K. 1987, *Nature*, **330**, 230
- [2] Fryer, C.L., Burrows, A., & Benz, W. 1996, *ApJ*, **496**, 333
- [Fryer & Heger 2000] Fryer, C. L., & Heger, A. 2000, *ApJ*, **541**, 1033
- [Hachisu et al. 1990] Hachisu, I., Matsuda, T., Nomoto, K., & Shigeyama, T. 1990, *ApJ*, **358**, L57
- [Herant & Benz 1992] Herant, M., & Benz, W. 1992, *ApJ*, **387**, 294

- [Höflich 1991] Höflich, P., 1991, *A&A*, **246**, 481
- [3] Hungerford, A. L., Fryer, C. L. & Warren, M. S., 2003, *ApJ*, in press
- [Janka & Mönchmeyer 1989] Janka, H.-T. & Mönchmeyer, R., 1989, *A&A*, **209**, L5
- [Kifonidis et al. 2000] Kifonidis, K., Plewa, T., Janka, H.-Th., Müller, E. 2000, *ApJ*, **531**, L123
- [] Khokhlov, A.M., Höflich, P.A., Oran, E.S., Wheeler, J.C., Wang, L., Chtchelkanova, A. Yu. 1999, *ApJ*, **524**, L107
- [Leonard & Filippenko 2001] Leonard, D. C., & Filippenko, A. V. 2001, *PASP*, **113**, 920
- [Mahoney] Mahoney, W. A., Varnell, L. S., Jacobson, A. S., Ling, J. C., Radocinski, R. G., & Wheaton, Wm. A. 1988, *ApJ*, **334**, L81
- [Matz et al. 1988] Matz, S. M., Share, G. H., Leising, M. D., Chupp, E. L., & Vestrand, W. T. 1988, *Nature*, **331**, 416
- [Mönchmeyer & Müller 1989] Mönchmeyer, R. & Müller, E., 1989, in *NATO ASI series, Timing Neutron Stars*, ed. H. Ögelman & E.P.J. van den Heuvel (New York: ASI)
- [Nagataki et al. 1998] Nagataki, S., Shimizu, T.M., & Sato, K. 1998, *ApJ*, **495**, 413
- [Pinto & Woosley 1988a] Pinto, P. A., & Woosley, S. E. 1988a, *ApJ*, **329**, 820
- [4] Spyromilio, J., Meikle, W. P. S., & Allen, D. A. 1990, *MNRAS*, **242**, 669
- [Tueller et al. 1990] Tueller, J., Barthelmy, S., Gehrels, N., Teegarden, B. J., Leventhal, M. & MacCallum, C. J. 1990, *ApJ*, **351**, L41